Atmospheric Acoustics

13

Dietrich Heimann, Arthur Schady and Joseph Feng

Abstract

This chapter deals with sound propagation in the atmosphere, which is an important link in the functional chain from noise emissions from aircraft, road and rail vehicles, and wind turbines to noise perception. The principle processes in outdoor sound propagation are explained. They include refraction, diffraction, and reflection. Two sound propagation models for scientific applications are briefly outlined. Finally, three illustrative applications and their results are discussed.

13.1 Introduction

The atmosphere is a carrier of various types of internal waves. Among them are sound waves which ensure aural communication between individuals, both people and animals. However, sound waves are also generated by technical devices, in particular those that move or have moving parts. Any kind of motorized means of transportation, such as aircraft, trains, trucks and cars, emits sound waves which

D. Heimann (✉) · A. Schady · J. Feng
DLR, Institute of Atmospheric Physics (IPA), Münchner Straße 20,
82234 Oberpfaffenhofen, Germany
e-mail: Dietrich.Heimann@dlr.de

A. Schady
e-mail: Arthur.Schady@dlr.de

J. Feng
e-mail: Joseph.Feng@dlr.de

U. Schumann (ed.), *Atmospheric Physics*, Research Topics in Aerospace,
DOI: 10.1007/978-3-642-30183-4_13,

propagate through the atmosphere. Such *sound*, once it is perceived by a human being, is often classified as *noise* because it is unwanted, annoying, disturbing, or even pathogenic.

Today, noise and above all traffic noise is seen as a severe environmental nuisance with psychological and physiological effects. Noise reduction is therefore a societal and political goal. This effort includes technical measures at the source to reduce noise *emissions* and measures influencing the propagation path, for instance the construction and installation of noise barriers. A solid knowledge of outdoor sound propagation effects is essential for assessing the noise situation in a given area and planning adequate and effective mitigation measures.

The Institute of Atmospheric Physics has dealt with the field of atmospheric *acoustics* and noise since the late 1990s. First, the activities were incorporated in aeronautics projects on quiet air traffic. Later, the activities were extended to transportation noise in general. A further extension to noise from wind turbines is envisaged.

In the following the principle processes and effects of outdoor *sound propagation* are summarized. A description follows of two model concepts which were implemented at the Institute of Atmospheric Physics. Finally, illustrative results of three applications (aircraft noise, sonic boom, influence of trees) are shown.

13.2 Outdoor Sound Propagation

Sound waves in the atmosphere consist of pressure oscillations associated with longitudinal particle motion, e.g. Embleton (1996), Ostashev (1997). A sound wave is characterized by its frequency f and sound pressure amplitude $\hat{p}$. For healthy young people the audible frequencies range from 16 Hz to 16 kHz with a maximum sensitivity between 1 and 6 kHz. The sound pressure amplitude is commonly expressed by the *sound pressure level* as a logarithmic measure $SPL = 10\lg\left(\hat{p}^2/p_0^2\right)$ dB (decibel) with $p_0 = 2 \cdot 10^{-5}$ Pa, the threshold of hearing at 1 kHz, as reference. The use of the squared sound pressure in the definition of *SPL* is a consequence of the fact that sound energy depends on the squared pressure amplitude. Hence, doubling the sound energy (e.g., two equal sound sources instead of one) raises the sound pressure level by approximately 3 dB because $\lg 2 \approx 0.3$. In practice the sound pressure level is often frequency-weighted to consider the human sensibility to different frequencies. The most common 'A-weighting' reduces the sound level for frequencies below 1 kHz and above 6 kHz according to the human capability of perceiving tones of different frequency.

In the atmosphere the sound speed mainly depends on the temperature T: $c \approx \sqrt{\kappa R T}$ with the ratio of specific heats $\kappa = c_p/c_v = 1.4$, and the gas constant of dry air $R = 287\,\mathrm{J\ kg^{-1}\,K^{-1}}$. Near the ground the sound speed relative to the air varies between 315 m/s and 350 m/s assuming typical mid-latitude temperatures. The *wavelength* is related to the speed of sound c and *frequency* f by $\lambda = c/f$. Hence, the wavelengths of audible frequencies cover a wide range from 2 cm to 20 m.

Outdoor sound propagation is affected by processes which depend on the actual state of the atmosphere, by interactions with the even or uneven ground, and with obstacles on the ground such as buildings, screens or vegetation. Before typical atmospheric propagation effects are illustratively described, the processes involved are first defined separately.

Geometrical spreading. Once a point source emits sound uniformly into the air space (spherical wave fronts), the sound intensity (i.e., the sound energy flux density) decreases proportional to $1/d^2$ where d is the distance from the source. This causes the *SPL* to decrease by approximately 6 dB as the distance doubles. In the case of a line source (cylindrical wave fronts), the *SPL* decreases proportional to $1/d$ or by approximately 3 dB as the distance doubles (because of $10\,\lg(1/2) \approx -3$).

Air absorption. The particle motion associated with sound waves causes friction, which converts a part of the sound energy into heat. Transversal and rotational vibration modes of two-atomic (e.g., O_2 and N_2) and three-atomic (e.g., H_2O) molecules lead to further losses of sound energy. As a consequence sound is attenuated with distance in addition to the effect of geometrical spreading. Air absorption depends on air pressure, temperature, and humidity. Generally, it is the stronger the higher the frequency. For a temperature of 15 °C, a relative humidity of 70 % and an air pressure of 1 000 hPa a 100 Hz wave is attenuated by only 0.25 dB/km, while a 5 kHz wave is attenuated by even 40 dB/km. Therefore, high frequency sound does not play a role beyond some 100 m.

Sound refraction. Refraction occurs if gradients of temperature T (and hence *sound speed* c) or *wind speed* U have a component perpendicular to the direction of propagation. In these cases the wave fronts change their direction, i.e., the sound does not propagate straight ahead (along straight sound rays), but follows a curve (curved sound rays) into the direction of lower temperature T or wind speed U. The curvature (inverse radius) is proportional to the atmospheric velocity gradients. In the near-ground atmosphere, i.e., in the *atmospheric boundary layer*, the gradients of c and U are strongest in the vertical direction. Here, horizontal sound propagation from near-ground sources to near-ground receivers is most affected by refraction. For noise from elevated sources like aircraft flying higher than some 100 m above ground, the effects of refraction occur only far away from the foot of the source. Unless the elevated source is very loud, e.g., sonic booms from supersonic aircraft, refraction effects are therefore of minor importance.

Sound diffraction. Diffraction occurs at convex surfaces or edges of obstacles where a part of the sound is directed into a shielded space. A typical example is diffraction at the top edges of a noise barrier, which allows noise to be diverted to the side of the barrier opposite to the source, i.e., into the protected zone. The longer the wavelength, the more effective is the diffraction.

Sound reflection. Airborne sound is fully or partly reflected at the ground surface or the surfaces of buildings, etc. Specular reflection occurs if the surface is plain with the angle of incidence being equal to the angle of reflection. At rough surfaces the reflection is diffuse. Reflectivity depends on the impedance of the

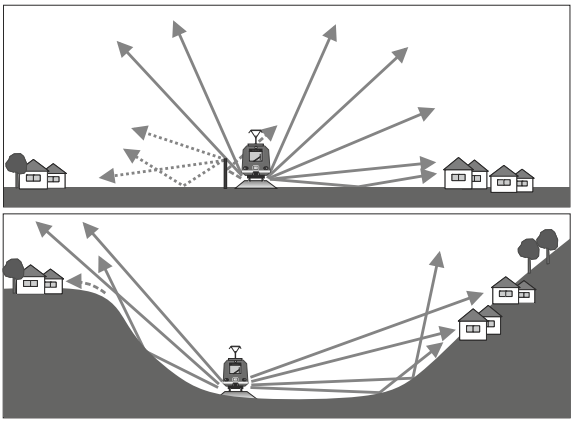

Fig. 13.1 Sound rays showing reflection at plane (*top*) and sloped (*bottom*) ground. Diffracted rays (behind a noise barrier and convex terrain) are broken

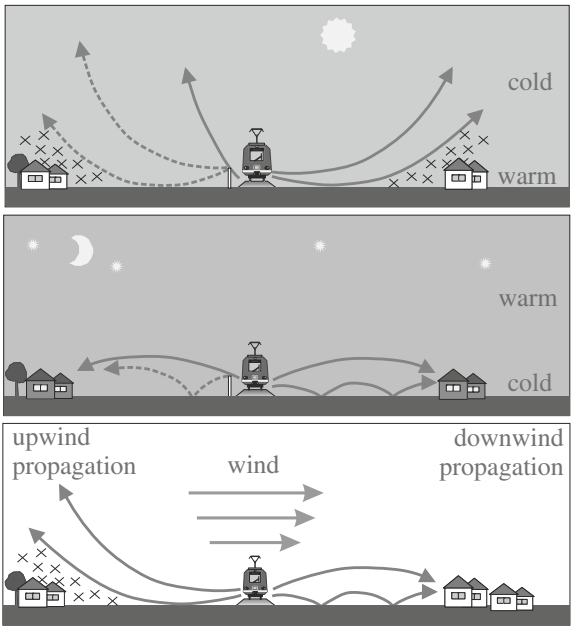

Fig. 13.2 Sound rays with upward refraction during daytime (*top*) and downward refraction during nighttime (*center*). The bottom panel shows upward and downward refraction in upwind and downwind propagation, respectively. Shadow zones are indicated by *crosses*, diffracted rays are drawn *dashed*

reflecting medium (e.g., the ground) relative to the impedance of air: $Z = \rho\, c$ with ρ being the air density. Solid media such as concrete have high impedance, causing strong reflection, while porous media (e.g., the soil) have low impedance, causing only weak reflection. In the case of grazing incidence in near-ground propagation over low impedance, porous ground, the reflected sound is phase shifted by 180°. Hence, the superposition of reflected and direct, non-reflected sound at the receiver causes destructive *interference* and low sound pressure amplitudes. Therefore, acoustically soft, i.e., low-impedance, porous ground or fresh snow leads to a high attenuation of near-ground to near-ground propagation. This damping effect gradually vanishes for steeper incidence.

Sound scattering. Turbulent eddies in the air whose extension is equal to or shorter than the wavelength cause a scattering of sound where forward and backward scattering is more important than sideward scattering. Besides turbulence, scattering is also caused by filigree obstacles like twigs and tree branches.

Typically, noise propagates over irregular ground (solid or porous, plane or hilly) with buildings and vegetation in an inhomogeneous atmosphere with temperature and wind gradients. Therefore, several of the aforementioned processes act in combination. Such combinations are illustrated in Figs. 13.1 and 13.2. They show typical situations of ground-to-ground propagation with a ground-based source (e.g., road or rail traffic, aircraft on runways) and ground-based receivers.

Behind a noise barrier or behind convex terrain an acoustical shadow forms where direct sound incidence is no longer possible. Only diffracted or scattered sound can enter this acoustical shadow.

Downward refraction typically occurs during night in the case of a temperature *inversion* (warm above cold air) with the sound speed increasing with height. Downward refraction also occurs in downwind propagation because the wind speed increases with height. Downward refracted sound is (repeatedly) reflected at ground, which leads to long-range audibility. By contrast, upward refraction occurs during the day when the temperature decreases with height or in upwind propagation. Beyond a certain distance from the source a shadow zone forms where audibility is strongly reduced.

13.3 Sound Propagation Modeling

Sound propagation models are typically used to predict the *SPL* due to given sources and propagation conditions in a selected domain. Various types of such models are published in the literature (Salomons 2001; Bérengier et al. 2003) and differ in the degree of sophistication. Rather simple models are used as noise prediction tools in engineering applications. More sophisticated ones are designed for scientific studies and specific applications. At the Institute of Atmospheric Physics two numerical sound propagation models of the latter type are used. Both models are capable of regarding the influence of meteorology and topography on sound propagation. However, they have specific advantages and disadvantages. The two models are briefly described below.

In the following, the atmospheric parameters are split into a mean part and deviations from that mean. So, we assume that the velocity vector $\mathbf{U} = \bar{\mathbf{U}} + \mathbf{U}' + \mathbf{U}''$ and the pressure $p = \bar{p} + p' + p''$ are each composed of a mean wind speed vector $\bar{\mathbf{U}}$ and a mean air pressure $\bar{p}$, with turbulent deviations from these means $\mathbf{U}'$ and p', and additional acoustical deviations describing the particle velocity vector $\mathbf{U}''$ and the sound pressure p''. Analogously, we may decompose the density ρ and the temperature T. The mean and turbulent parts can be combined to define the meteorological background state ($p_{met} = \bar{p} + p'$, $\mathbf{U}_{met} = \bar{\mathbf{U}} + \mathbf{U}'$, $\rho_{met} = \bar{\rho} + \rho'$, and $T_{met} = \bar{T} + T'$) of the acoustical waves.

Sound Particle Model

This model is based on ray acoustics (Heimann and Gross 1999). At the source a large number of virtual 'sound particles' are emitted into the environment. Each particle is associated with a partial sound energy which is distributed to frequencies according to the acoustic source spectrum. These particles travel with the local sound speed c along sound rays. In the absence of wind or temperature gradients the rays are straight (no refraction). They are curved in the presence of wind or temperature gradients (refraction).

The vector of position $\mathbf{X}_i$ of the ith sound particle and its associated wave front unit vector $\mathbf{N}_i$ are given by

$$\frac{\partial \mathbf{X}_i}{\partial t} = \mathbf{U}_{met} + c\,\mathbf{N}_i \tag{13.1}$$

$$\frac{\partial \mathbf{N}_i}{\partial t} = -\nabla c - \mathbf{N}_i \cdot \nabla \mathbf{U}_{met} \tag{13.2}$$

These equations are integrated in time for each particle until it has left the model domain. Once a particle hits the ground or an obstacle it is reflected (specular reflection at plain surfaces or diffuse reflection at rough surfaces). According to the impedance ratio and the angle of incidence the phase is shifted and a part of its attributed energy is lost.

All particles which are passing receiver points within a defined distance are counted and their respective complex sound pressures (indicating amplitude and phase) are added up to calculate the local sound pressure level *SPL*.

The Lagrangian sound particle model is best suited to high-frequency sound. Diffraction cannot be modeled straightforwardly, but needs special treatments.

Finite-Difference Time-Domain Model

The sound waves that propagate through the atmosphere can be well described by linear acoustics. Nonlinear effects are limited to the near-field of a strong acoustical source or to acoustical shock waves such as sonic booms. A linearization of the Euler equation of motion and the equation of continuity with respect to a given meteorological background, neglecting non-adiabatic processes, Earth's rotation, internal friction and gravitation, leads to a set of prognostic equations for the particle velocity $\mathbf{U}''$ and the sound pressure p'' (Heimann and Blumrich 2002; Salomons et al. 2002; Heimann and Karle 2006). A scale-analysis suggests the negligibility of further terms so the prognostic equations of sound waves read:

$$\frac{\partial p''}{\partial t} = -\mathbf{U}_{met} \nabla p'' - \kappa\, p_{met} \nabla \cdot \mathbf{U}'' \tag{13.3}$$

$$\frac{\partial \mathbf{U}''}{\partial t} = -\mathbf{U}_{met} \nabla \mathbf{U}'' - \frac{1}{\rho_{met}} \nabla p'' \tag{13.4}$$

This set of prognostic equations describes geometrical spreading, refraction, and diffraction. Reflection is considered by appropriate boundary conditions. The equations are numerically integrated in time within a two- or three-dimensional computational domain. Depending on the numerical scheme the cell size of the numerical grid has to be smaller than five to ten times the acoustical wavelength. The sound pressure amplitude is evaluated at the receiver cells and the sound pressure level *SPL* is determined.

The *Eulerian finite-difference time-domain model* is universal and very efficient for low-frequency sound. Long-range simulations of high-frequency sound are often limited by the available computational resources.

13.4 Applications

Sound propagation models can be applied to various problems in atmospheric acoustics. At the Institute of Atmospheric Physics applications included noise propagation in valleys (Heimann and Gross 1999; Heimann et al. 2010) and street canyons (Heimann 2007), interactions with slope (Heimann 2006, 2010), flow and turbulence behind noise barriers (Heimann and Blumrich 2002, 2004), scattering and reflection by trees (Heimann 2003), noise of aircraft during takeoff and landing (Neise 2007), sonic booms from supersonic aircraft (Heimann 2001; Blumrich et al. 2005a, b; Kästner and Heimann 2010), and the role of wake flow behind wind turbines (Heimann et al. 2011). In addition, considerations were made how meteorological conditions can be categorized for sound propagation modeling (Heimann and Salomons 2004; Defrance et al. 2007; Heimann et al. 2007). Three of these applications and their results are discussed in the following.

Noise of Aircraft During Takeoff

Noise in the neighborhood of *airports* is an important issue which often leads to night-flight bans or limitations on the allowed number of operations. Successful efforts to reduce noise by introducing new, less noisy aircraft were often compensated or even overcompensated by the increasing number of flights. Moreover, replacing an aircraft fleet with modern low-noise vehicles takes a rather long time. Therefore, the noise reducing potential of alternative operational procedures is investigated, too. Above all, these are low-noise approach and departure procedures, e.g., continuous descent approaches, steep flight profiles during landing, or reduced power settings during takeoff. In summer 2006 flight tests with different approach and departure procedures were performed in cooperation with Lufthansa

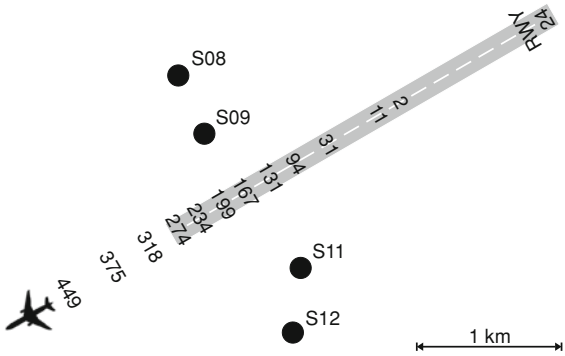

Fig. 13.3 Sketch of runway 24 at Parchim airport and the positions of the four receivers (S08, S09, S11, S12) mentioned in the text. The numbers along the aircraft track indicate the altitude of the departing aircraft in meters above ground

at Parchim airport near Schwerin (Neise 2007). A large number of sound level meters were installed to measure the noise.

Here a part of these data are used to validate sound propagation simulations with the sound particle model described above. Four measurement stations (receivers) were installed perpendicular to the center line of the runway at different distances (Fig. 13.3). The noise was measured during the takeoff of an Airbus A310 twin-jet passenger aircraft at 1.5 m above ground. As the aircraft passed, noise from different angles of sound radiation was encountered by the receivers. Therefore, the noise emission and the emission frequency spectrum were considered as functions of this angle. Figure 13.4 shows how the noise level varies as a function of the azimuth angle under which the departing aircraft is seen from the receiver during the flyby (full-thrust takeoff procedure). While the aircraft climbs and moves against the wind towards the southwest, the outer receivers (S08 and S012) soon come out of the initial acoustical shadow caused by upward refraction during near-ground upwind propagation. Except for the time in the acoustical shadow, the coincidence of measurements and model results is fairly good.

In Fig. 13.5 the observed and simulated spectra are shown for three aircraft positions, given by the azimuth angle under which the aircraft is seen from the receiver during the flyby. Since different aircraft positions also mean different emissions angles, the emission spectra vary. The spectra at the receivers deviate from the emission spectra because of frequency-dependent air absorption and ground reflection which cause partly destructive, partly constructive interference of direct and reflected sound, depending on frequency. Measured and simulated spectra at the receivers are in good agreement.

Sonic-Boom Propagation

Supersonic aircraft flying with a speed V greater than the speed of sound c (i.e., *Mach number* $M = V/c > 1$) generate a shock wave which produces a loud bang near the ground, the "*sonic boom*." The sonic boom is not only very annoying to people, but also a threat to animals, including marine mammals. The discussion to

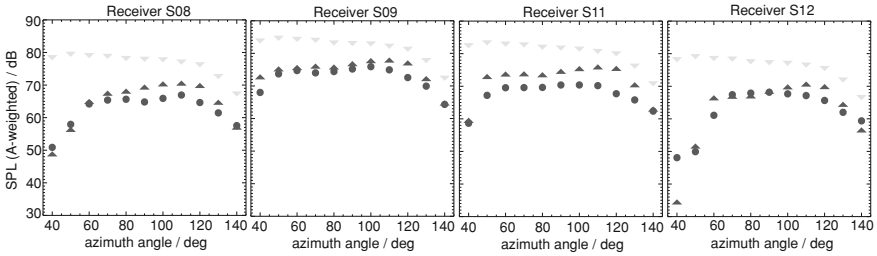

Fig. 13.4 Sound pressure level during flyby at the four receivers shown in Fig. 13.3. The abscissa provides the azimuth angle under which the aircraft is seen from the respective receivers (0° front view, 90° side view, 180° back view). The *bullets* indicate the measurements. The *dark triangles* show the model results. Measurements and model results are for 1.5 m above ground. The *light triangles* provide the emission levels (lateral directivity). All sound levels are A-weighted

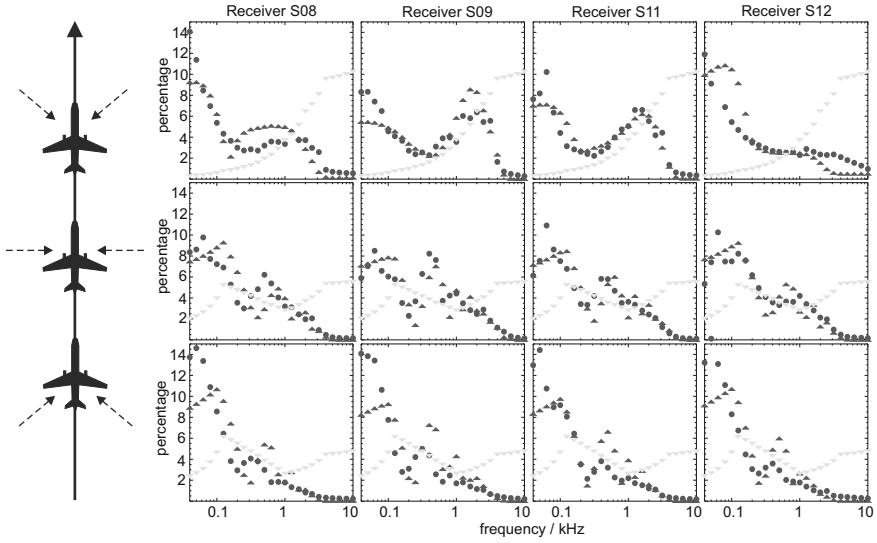

Fig. 13.5 Observed (*bullets*) and simulated (*dark triangles*) spectra at the four receivers shown in Fig. 13.3 (1.5 m above ground). The upper, middle and lower rows are for an azimuth angle of 40°, 90°, and 140°, respectively, under which the aircraft is seen from the receivers (*dashed arrows* on the *left*). The *light triangles* provide the emission spectrum

(re)introduce supersonic passenger or business aircraft brought about several research projects to investigate the potential environmental problems of intensive supersonic air traffic and to explore possible solutions. The sonic-boom problem was especially addressed. One study in this context aimed at the identification of specific refractive atmospheric situations and flight parameters which prevent the sonic boom from reaching the ground (Kästner and Heimann 2010).

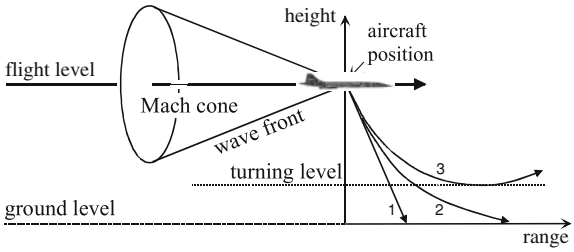

Fig. 13.6 Schematic view of the Mach cone and three sonic-boom sound rays: *1*: non-refracted straight ray reaching the ground, *2*: upward refracted ray reaching the ground, *3*: upward refracted ray not reaching the ground. Taken from Kästner and Heimann (2010)

The sonic-boom shock wave front is defined by the *Mach cone* (Fig. 13.6) and propagates perpendicular to the Mach cone surface. The initial direction of sonic boom propagation of an aircraft flying only marginally faster than 1 Mach is only slightly slanted towards the ground. The faster the aircraft, the steeper the downward direction of sonic-boom propagation. Normally, supersonic vehicles fly at high altitudes between 15 and 25 km, i.e., in the middle stratosphere. During downward propagation the orientation of the wave front changes by refraction depending on the wind and temperature gradients encountered. Important atmospheric features between typical supersonic flight levels and ground are the wind maximum of the jet stream and the tropopause with its characteristic kink in the vertical temperature gradient. Under certain circumstances it may happen that sonic-boom sound rays are refracted upward so that they turn and do not reach the ground. In such cases the sonic boom would not be heard at ground ('no boom') or would at least not be very loud ('low boom').

How frequently a sound boom does not reach the ground depends on many factors, viz. terrain height, regional climatology (frequency distributions of wind and temperature profiles), and relevant flight parameters (altitude, speed or Mach number, heading). An example of calculated sonic-boom sound rays (with Eqs. 13.1 and 13.2) is shown in Fig. 13.7. The chance of a sonic boom not reaching the ground is especially high if the Mach number is low ($M < 1.2$) because in that case the rays start in a nearly horizontal direction and are most affected by refraction due to vertical gradients. The chance is also increased for flight directions against the mean wind direction and for low terrain elevations. Figure 13.8 provides the regional distribution of the frequency of occurrence of low or no boom situations in Europe for a specific set of flight parameters.

Influence of a Tree on Sound Propagation

Single trees, rows of trees or forests influence sound propagation, directly through reflection and scattering of sound wave by trunks, branches and twigs, and/or indirectly through modified refraction due to the influence of the trees on the wind

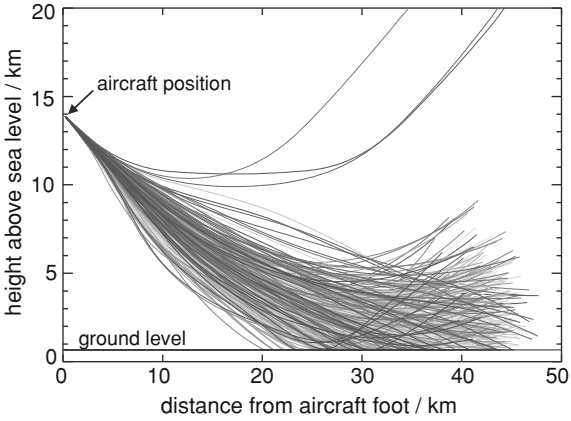

Fig. 13.7 Calculated daily sound rays for the year 2001 at Munich for a westward-heading aircraft flying at 1.2 Mach at 14 km altitude. Taken from Kästner and Heimann (2010)

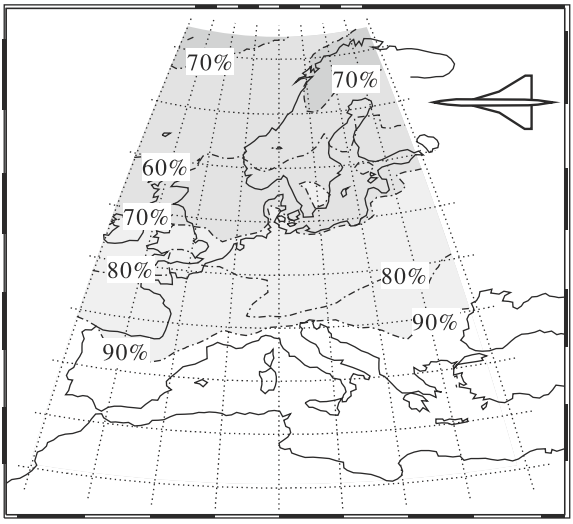

Fig. 13.8 Frequency distribution of low or no boom situations (turning level above ground) for the period 1991–2001 for supersonic flights of 1.15 Mach at 15.2 km altitude and westward headings. Taken from Kästner and Heimann (2010)

field. Many studies have been undertaken to quantify the influence of trees. These include theoretical considerations (e.g., scattering by cylinders), measurements and model simulations. With the finite-difference time-domain model (Eqs. 13.3 and 13.4) it is possible to resolve the tree trunk and major branches in three dimensions. The model is capable of simulating reflection (wavelengths smaller than the trunk/branch diameter) as well as scattering (wavelength equal or larger than the diameter).

To investigate the influence of a row of single trees, a 30 m long, 8 m wide and 24 m high model domain with a numerical resolution of 0.05 m was defined. The resolution allows the evaluation of spectra for $f \leq 1350\,\mathrm{Hz}$. Hence, the domain consists of 46 million numerical grid cells. A 16 m high idealized tree (a vertical straight trunk with straight branches) with a crown diameter of 8 m was placed in the center of the domain. Two arrays of virtual receivers were placed 3 m in front

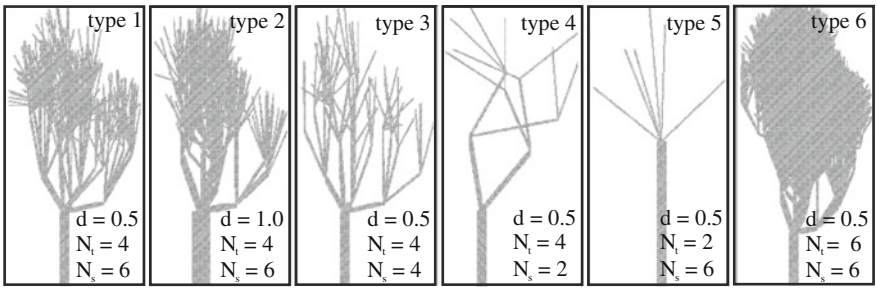

Fig. 13.9 Silhouettes of idealized trees (only trunk and branches) with different parameter settings (d: diameter of the trunks in m, N_t: number of branching orders, N_s: number of branches per branching order). The branch diameter halves per branching sequence. All trees are 16 m high with a crown diameter of 8 m

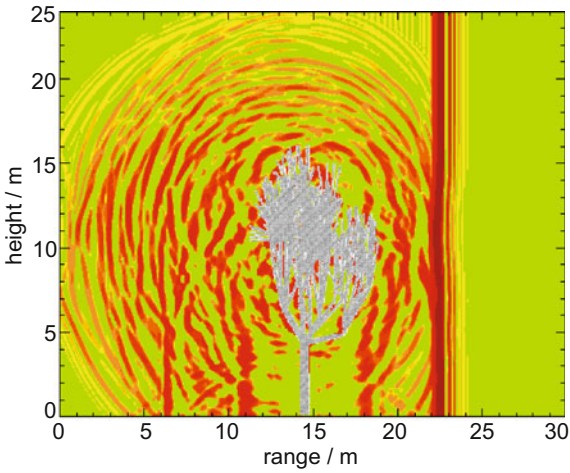

Fig. 13.10 Snapshot of simulated sound pressure (vertical cross-section through the center of the domain) after the wave front has passed an idealized row of trees (type 1; silhouette in *grey*) from *left* to *right*

and 3 m behind the tree. At these arrays the backscattered or backward reflected sound and the forward transmitted sound are recorded. Cyclic boundary conditions in the lateral directions suggest the existence of an infinite row of trees. The chosen simulation time of 0.09 s ensures that besides the signal of the center tree at least the sideward scattered or reflected sound from the adjacent trees is recorded at the arrays. The scattered and reflected signals of farther distant trees do not much contribute anyway.

The simulations were performed for six types of trees (Fig. 13.9). Trunks and branches are assumed to be cylinders. The parameters characterizing the tree type include the trunk diameter d, the number of branching orders N_t, and the number of branches per branching order N_s. The first order branches have a diameter that is half of the trunk diameter, the branch diameter again halves from one order to the subsequent one. For each parameter setting five random realizations were simulated. They differ by the random orientation of the branches.

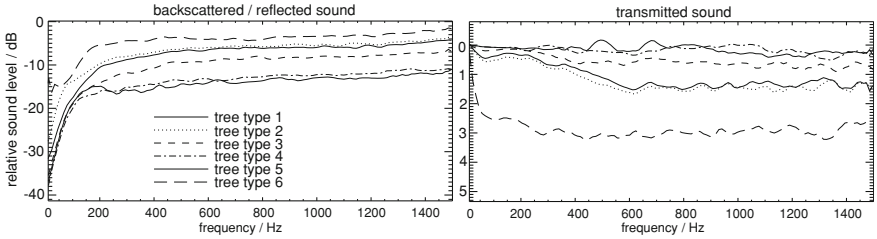

Fig. 13.11 Spectral distribution of backscattered and backward reflected sound (*left*) and of transmitted sound (*right*). The results are shown for six types of idealized trees. The sound levels are relative to the undisturbed sound. Note the different scales at the vertical axes

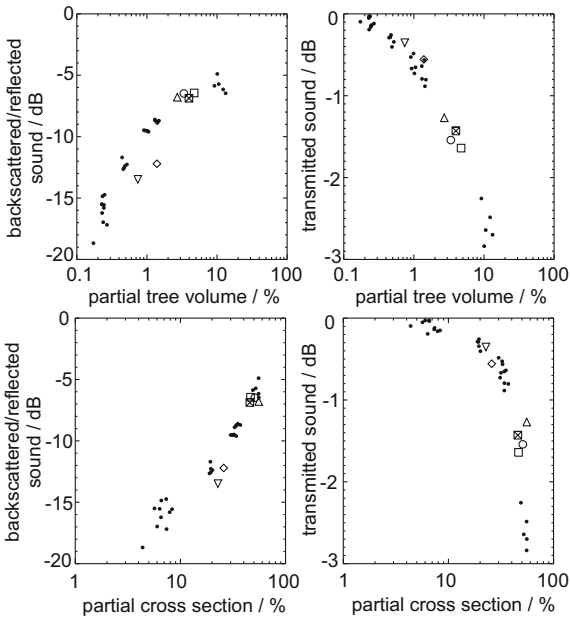

Fig. 13.12 Simulation results of backward directed (*left*) and transmitted (*right*) sound relative to undisturbed sound as a function of partial tree volume (*top*) and partial cross section (*bottom*). The *dots* refer to the six tree types with five realizations per type. Other symbols refer to six different sets of laser-scan tree data (courtesy of A. Bienert, Professur für Photogrammetrie, TU Dresden)

In the model simulations a plane upright sound pressure pulse, oriented parallel to the row of trees, propagates horizontally and penetrates the tree. As an example Fig. 13.10 provides a vertical cross section of the sound pressure field perpendicular to the row of trees after the pulse has passed the row. While the pulse front itself is hardly distorted, irregular patterns around the tree indicate that sound is scattered and reflected in all directions.

Signal evaluation at the receiver arrays in front of and behind the row of trees reveals that low-frequency sound ($f \leq 100\,\mathrm{Hz},\ \lambda \geq d$) is hardly directed backward and passes the row of trees without significant hindrance (Fig. 13.11). The degree of reflection and transmission of medium and high frequency sound depends on the chosen tree parameters.

Figure 13.12 shows the result for all model simulations with various types of trees. Here the trees are characterized by the ratio of wood to air in the enveloping tree volume and in the silhouette as seen from the approaching sound wave. The results suggest a functional relationship between these parameters on the one side and the backward and forward sound energy on the other side. This relationship can be used for the parameterization of trees in simulations which do not permit the resolution of single trees.

13.5 Conclusions and Outlook

Atmospheric acoustics provides knowledge and tools to describe the propagation of sound in the atmosphere. For the solution of outdoor noise problems, in particular noise from aircraft, road vehicles, trains and wind turbines, sound propagation is an important link between source and receiver. It is part of the functional chain between noise emission and noise effects on human beings (e.g., sleep disturbance, annoyance, impairment of heath). While state-of-the-art noise prediction tools are regulated in national and international standards (e.g., ISO 9613-2 (1996)) scientific sound propagation models are much more sophisticated and are capable of describing meteorological and topographical influences in physical detail. However, these models are rather demanding in terms of computational resources, both as to time and storage. Therefore, the use of these models is limited to scientific applications (investigations of processes and relationships, for instance to derive parameterizations) and selected practical problems.

Nevertheless, there is still a high potential for new fields of application and further development of the models. The availability of more powerful computers in future will open applications to larger ranges and higher frequencies. Another extension of applicability is expected from the introduction of refined numerical techniques.

References

Bérengier, M.C., Gauvreau, B., Blanc-Benon, P., Juvé, D.: Outdoor sound propagation: a short review on analytical and numerical approaches. Acta Acust. **89**, 980–991 (2003)

Blumrich, R., Coulouvrat, F., Heimann, D.: Variability of focused sonic booms from accelerating supersonic aircraft in consideration of meteorological effects. J. Acoust. Soc. Am **118**, 696–706 (2005a). doi:10.1121/1.1938547

Blumrich, R., Coulouvrat, F., Heimann, D.: Meteorologically induced variability of sonic-boom characteristics of supersonic aircraft in cruising flight. J. Acoust. Soc. Am. **118**, 707–722 (2005b). doi:10.1121/1.1953208

Defrance, J., Salomons, E., Noordhoek, I., Heimann, D., Plovsing, B., Watts, G., Jonasson, H., Zhang, X., Premat, E., Schmich, I., et al.: Outdoor sound propagation reference model developed in the European Harmonoise project. Acta Acust. **93**, 213–227 (2007)

Embleton, T.F.W.: Tutorial on sound propagation outdoors. J. Acoust. Soc. Am. **100**, 31–48 (1996)

Heimann, D.: Effects of long-term atmospheric variability on the width of a sonic-boom carpet produced by high-flying supersonic aircraft. Acoust. Res. Lett. **2**, 73–78 (2001)
Heimann, D.: Numerical simulations of wind and sound propagation through an idealised stand of trees. Acta Acust. **89**, 779–788 (2003)
Heimann, D.: Sound propagation in a nocturnal slope-wind layer—a numerical model study. Acta Acust. **92**, 362–369 (2006)
Heimann, D.: Three-dimensional linearised Euler model simulations of sound propagation in idealised urban situations with wind effects. Appl. Acoust. **68**, 217–237 (2007)
Heimann, D.: On the efficiency of noise barriers near sloped terrain—a numerical study. Acta Acust. **96**, 1003–1011 (2010). doi:10.3813/AAA.918363
Heimann, D., Blumrich, R.: Anwendungsbeispiele numerischer Schallausbreitungssimulationen mit konsistenter Berücksichtigung der Atmosphäre. Z. Lärmbekämpfung **49**, 91–97 (2002)
Heimann, D., Gross, G.: Coupled simulation of meteorological parameters and sound intensity in a narrow valley. Appl. Acoust. **56**, 73–100 (1999). doi:10.1016/S0003-682X(98)00018-1
Heimann, D., Blumrich, R.: Time-domain simulations of sound propagation through screen-induced turbulence. Appl. Acoust. **65**, 561–582 (2004). doi:10.1016/j.apacoust.2003.09.007
Heimann, D., Karle, R.: A linearized Euler finite-difference time-domain sound propagation model with terrain-following coordinates. J. Acoust. Soc. Am. **119**, 3813–3821 (2006).doi: 10.1121/1.22000139
Heimann, D., Salomons, E.: Testing meteorological classifications for the prediction of long-term average sound levels. Appl. Acoust. **65**, 925–950 (2004). doi:10.1016/j.apacoust.2004.05.001
Heimann, D., Bakermans, M., Defrance, J., Kühner, D.: Vertical sound speed profiles determined from meteorological measurements near the ground. Acta Acust. **93**, 228–240 (2007)
Heimann, D., Schäfer, K., Emeis, S., Suppan, P., Obleitner, F., Uhrner, U.: Combined evaluations of meteorological parameters, traffic noise and air pollution in an Alpine valley. Meteorol. Zeitschrift **19**, 47–61 (2010). doi:10.1127/0941-2948/2010/0426
Heimann, D., Käsler, Y., Gross, G.: The wake of a wind turbine and its influence on sound propagation. Meteorol. Zeitschrift **20**, 449–460 (2011). doi:10.1127/0941-2948/2011/0273
ISO 9613-2: Acoustics—attenuation of sound during propagation outdoors. Part 2: General method of calculation (1996)
Kästner, M., Heimann, D.: Effect of atmospheric variability and aircraft flight parameters on the refraction of sonic booms. Acta Acust. **96**, 425–436 (2010). doi: 10.3813/AAA. 918295
Neise, W. (ed.): Lärmoptimierte An- und Abflugverfahren. Zusammenfassender Schlussbericht (2007)
Ostashev, V.: Acoustics in Moving Inhomogeneous Media. E.&F.N. Spon, London (1997)
Salomons, E.: Computational Atmospheric Acoustics. Kluwer, Norwell (2001)
Salomons, E., Blumrich, R., Heimann, D.: Eulerian time-domain model for sound propagation over a finite-impedance ground surface. Comparison with frequency-domain models. Acta Acust. **88**, 483–492 (2002)